Journal of Applied Mechanics and Technical Physics, Vol. 38, No. 1, 1997

MODELING OF SHOCK-WAVE COMPACTION OF POWDER CERAMICS USING A BALLISTIC TESTING UNIT

N. N. Belov, A. A. Konyayev, P. V. Korolyov, S. N. Kul'kov, A. G. Mel'nikov, T. M. Platova, V. G. Simonenko, V. F. Tolkachyov, and M. V. Khabibullin

UDC 539.3+621.7.044.2

The problem of creation of high-density compacts from raw material in ultradispersed ceramic powder is considered. In many cases, preliminary treatment of powders of refractory compounds by pulsed pressure substantially facilitates further formation of compact products by the methods of powder metallurgy [1, 2]. On the one hand, shock-wave compression of nanocrystallite submicron ceramics leads to a qualitative change in the morphology and to fragmentation of the powder particles: the bulk density increases, and additional saturation of the particles by defects of the crystalline structure is observed. The accumulated strain energy increases in the powder and polymorphous conversions occur. On the other hand, the possibility arises of obtaining, immediately in the shock wave, large agglomerates or one-piece compacts of particles, with a density close to that of a monolith. In both cases, it is necessary to know the optimal regimes of shock-wave treatment, because it is known that, for example, the degree of defectiveness and the area of the particle surface are the functions of pressure. As the intensity of the shock wave increases, bonding of the crystalline powder goes through a maximum, and under very strong loadings monolithic compacts are difficult to obtain because of dislocation breakdown of the lattice.

The physicomechanical and chemical properties of new modifications of nanocrystallite ceramics depend not only on the amplitude of shock compression, but also on many other factors, including the load rate and duration and pressure gradients in unloading waves. It can be expected that, having constructed an optimal stress–time diagram, one can obtain the required modifications of submicron ultradispersed powders at various structural levels and form sufficiently dense homogeneous compacts with an acceptable concentration of defects in the powder. However, selection of optimal regimes of shock-wave compaction is by no means easy, because the pulsed compaction of powders is often multidimensional and nonstationary, and the set of kinematic and dynamic parameters of it is difficult to record experimentally over a wide time interval. The pressure amplitude at the wall of a conservation ampoule is, as a rule, an estimate that is accessible to determination and sufficiently reliable.

One of the methods of finding the optimal parameters of shock-wave compression is to obtain quantitative information on the evolution of the stress-strain state on the basis of simulation of the dynamics of powder compaction with an appropriate experimental testing for model adequacy at the reference points of the initial and final compaction stages.

In the present paper, we present the results of an experimental-theoretical investigation of shock-wave compaction of the powder of ultradispersed tetragonal zirconium dioxide using a ballistic test unit. Pulsed loading of the powder using a ballistic test unit is of interest, because the stress–time diagram can be varied widely in time, with variation in the impact velocity, mass, length, and material of an accelerated striker. Powder compaction in a cylindrical conservation ampoule is reached at the initial stage as a result of the action of a traveling compression wave, and then as a result of the increased loading because of multiple reflection of stress waves from mobile and immobile punches. The kinematic parameters of a single compression in the conservation ampoule were recorded in a series of experiments by the method of needle sensors placed in a

Institute of Applied Mathematics and Mechanics, Tomsk 634050. Translated from Prikladnaya Mekhanika i Tekhnicheskaya Fizika, Vol. 38, No. 1, pp. 43–50, January–February, 1997. Original article submitted June 22, 1995; revision submitted August 9, 1995.

 0021-8944/97/3801-0038 $18.00

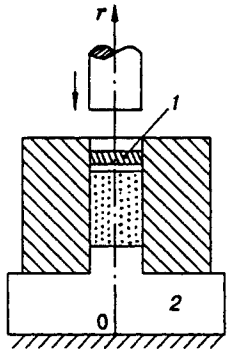

Fig. 1

TABLE 1

Powder composition	a, mm	$\langle\sigma\rangle$	b, mm	$\langle\sigma\rangle$	h, mm	$\langle\sigma\rangle$
In the double ZrO_2–Y_2O_3 system after compaction	2.7	0.9	4.1	1.4	—	—
In the double ZrO_2–Y_2O_3 system after annealing at 1200°C during 1 h in vacuum	3.9	0.9	5.4	1.5	1.0	0.4
In the triple ZrO_2–Y_2O_3–Al_2O_3 system after annealing at 1200°C during 1 h in vacuum	7.8	2.3	12.1	2.8	0.7	0.3

sample, i.e., in a low-dense medium [3]. The final density of the compacted preform served as a reference point to find kinetic constants in the mathematical model of powder compaction.

Experimental Procedure. A steel cylindrical striker was accelerated with a powder ballistic gun of 23 mm. The impact velocity ranged from 0.3 to 2 km/sec. The velocity of the striker was recorded by the electrocontact method with an error of 1.5%. The conservation ampoule was a thick-walled knock-down cylinder made of high-strength steel (Fig. 1). The cylinder was fastened to the barrel of the ballistic unit. The powder to be investigated was placed into the ampoule, and mobile (1) and immobile (2) punches were placed on the ends. A flat side impact by the cylinder was given to the mobile steel punch. Fragmentation and compaction of the powder to be studied were performed by direct and reflected compression waves in the space between the mobile and immobile punches upon movement of the striker into the conservation ampoule. The maximum pressure of the mobile punch was 5–43 GPa in the investigated velocity range of the striker.

As the original material, we used the 97 mol.% ZrO_2 + 3 mol.% Y_2O_3 powder produced by thermal decomposition of salt solutions dusted in a high-frequency plasma (by plasmochemical synthesis). During this process, a drop of solution transforms into a solid powder particle in approximately 1 sec. As a result, the powder particles are void spheres or their fragments with an average diameter of 0.25 μm. The size of such a powder particle corresponds to the diameter of the drop solution from which it was produced. The unusual morphology of the particles is also explained by this circumstance. X-ray data show that the powder is in the tetragonal phase immediately after its production. An x-ray analysis of all the samples was made using a DRON-UM1 diffractometer with copper- or cobalt-filtered radiation. Recording was made at the points with the number of pulses such that an error of less than 0.05% was attained. The diffractograms obtained (in particular, selection of an x-ray line of the profile, determination of its half-width, integral intensity, angular position, etc., with an accuracy of up to 1% or less) were processed with a computer program. The phase content of the powder is calculated by a standard procedure.

After shock-wave compaction, the sample was taken out of the ampoule, and the average density of the compacted material was determined. In addition to diffractometric analysis, all the powders were investigated with a "TESLA-BS-500" electronic microscope with an accelerating voltage of 90 kV. The samples for microscopic analysis were prepared by the replica method: the finest particles of the powder are first

deposited on glass, and a thin carbon film was then sprayed. The maximum fragmentation of hollow spheres occurred in the 250–500 m/sec range of impact velocities. With an increase in the initial velocity up to approximately 650 m/sec, the thickness of the compacted preform decreases. When the loading rate was further increased, the material of the preform laminated. The majority of the preforms extracted from the conservation ampoules were covered with a net of microcracks both in the plane of compaction and in the direction of pressure action. These microcracks, which are intercrystallite fractures, are seen more distinctly when the annealing temperatures are low.

Table 1 gives the linear dimensions of microcracks: a and b are the average dimensions of fragments in the plane of compaction, h is the average dimension of the fragments along the direction of pressure application, and $\langle\sigma\rangle$ is the variance. The triple ZrO_2–Y_2O_3–Al_2O_3 system represents a ZrO_2 powder during the synthesis of which ~20% of Al_2O_3 was added. With the total 35-g mass of the striker and the driving device and a powder mass of 10 g, the localization of microcracks in the direction of loading makes it possible to separate 3–4 layers with a thickness of 1–2 mm in the compacts. The volume occupied by the powder in the ampoule reduces upon compression by an order of magnitude: the average density of the compacted preform is 4.9 g/cm^3 at an initial density of the powder of 0.4 g/cm^3 for an impact velocity of 500 m/sec.

As in the case of explosion compression, after impact loading the morphology of particles in the ZrO_2–Y_2O_3 and ZrO_2–Y_2O_3–Al_2O_3 systems changes in a cardinal manner: practically no coarse particles remain in the powder medium, and the particle-size distribution is close to the crystallite-size distribution [2]. In the initial state, the average particle size determined by the data of electronic microscopy is 250 nm, and the size of crystallites in them is 12 nm, and after the action of impact they are 60 and 12 nm, respectively.

According to the data of x-ray analysis, the phase composition changes in a similar way: if the original powder contains 100% of the tetragonal phase (in accordance with the state diagram for ZrO_2–Y_2O_3), after the impact action in a velocity range of 500–1000 m/sec its content was decreased approximately by 60%, and the monoclinic phase appeared. The x-ray lines become noticeably wider. The amount of the monoclinic phase formed is maximal at pressures of 5–10 GPa, and the amount of the BCC form increases monotonically with increasing pressure. The BCC phase has been shown to be formed on the basis of a high-temperature modification of zirconium, and its appearance is apparently associated with considerable displacements of ions from the equilibrium state at the shock-wave front. Shock-wave treatment has been established to increase substantially the reactivity of the plasmochemical ZrO_2 powder upon low-temperature sintering. In particular, the grain size in the sintered samples is close to the crystallite size typical of the ceramics made from stabilized zirconium dioxide with the martensite reinforcement mechanism. This mechanism was not yet realized in full measure because of the high porosity of the sintered products. If one manages to control the sintering process of such active powders, ceramics with extremely high mechanical characteristics can be produced.

Formulation of the Problem. Shock compression of tetragonal zirconium dioxide stabilized by yttrium oxide leads to polymorphous conversions with a change in the volume. In the case of a tetragonal-monoclinic conversion ($t \rightleftarrows m$), the volume ranges from 4 to 9%. [4]. Thus, lamination of compacts due to the action of unloading waves can be complicated by fracturing because of the volume change at the $t \rightleftarrows m$ transition. With this in mind, the processes of shock compaction of a powder material and failure of a compacted preform should be calculated within the framework of the model of a porous elastoplastic material, whose matrix experiences a polymorphous phase transition under deformation [5].

Upon compaction of bulk materials, we shall model the actual medium, which is represented by solid particles with the forces of dry friction acting between them and by void spaces, as a spherical solid particle of a material subject to the Mohr–Coulomb condition. This makes it possible to derive a kinetic equation for powder compaction from solution of the problem of deformation of a spherical pore under the influence of an isotropic stress. Lack of information on the $t \rightleftarrows m$ transition does not allow one to construct a kinetic equation to calculate the mass concentration of the phases. Therefore, the processes occurring upon shock-wave treatment of powder zirconium dioxide in a rigid conservation ampoule were investigated within the framework of the model of a porous elastoplastic material.

Under the assumption that the pores remain spherical in the process of deformation, for nonstationary

flows with a single spatial variable r in the plane case, the basic equations have the form

$$\rho_0 \dot{u}/V = \partial \sigma_r/\partial r; \tag{1}$$

$$\dot{V}/V = \partial u/\partial r; \tag{2}$$

$$\dot{E} = VS_r \partial u/\partial r - (p+q)\dot{V}; \tag{3}$$

$$p = \frac{\alpha_0 \gamma_{0m} E}{\alpha} + \frac{\rho_{0m} c_{0m}^2 [1 - 0.5\gamma_{0m}(1 - \alpha_0 V/\alpha)](1 - \alpha_0 V/\alpha)}{\alpha[1 - s_{0m}(1 - \alpha_0 V/\alpha)]^2}; \tag{4}$$

$$2\mu_m(\partial u/\partial r - \dot{V}/3V)(1 - \dot{\alpha}V/\alpha\dot{V}) = \dot{S}_{rm} + \lambda S_{rm}. \tag{5}$$

Here the quantities with the subscript m refer to the material of the matrix, and those without the subscript refer to the porous material; u is the mass velocity, $\sigma_r = -(p+q) + S_r$ is the component of the stress tensor, p is the pressure, q is the artificial viscosity, $S_{rm} = \alpha S_r$ is the component of the stress tensor deviator, $\alpha = \rho_m/\rho$ is the porosity, ρ is the density, $V = \rho_0/\rho$ is the specific volume, $\rho_0 = \rho_{0m}/\alpha_0$ is the initial density, α_0 is the initial porosity, E is the internal energy per unit initial volume, γ_{0m} is Grüneisen's coefficient, μ_m is the shear modulus, and c_{0m} and s_{0m} are the coefficients in a linear dependence of the shock-wave velocity on the mass velocity.

The parameter λ is identically equal to zero in the elastic area. In the area of plastic flow, λ is found using the Mises yield condition

$$S_{rm}^2 = \frac{4}{9}\sigma_{sm}^2 \tag{6}$$

(σ_{sm} is the dynamic yield point). The process of plastic filling of pores is determined by the relations

$$\dot{\alpha} = 0, \quad 0 \leqslant p \leqslant p_{c1};$$

$$Y_0 \tau_1^2 Q_1(\alpha, \dot{\alpha}, \ddot{\alpha}) = \alpha p + Y_0\left[1 - \left(\frac{\alpha}{\alpha - 1}\right)^{2k/3}\right]\Big/k, \quad p > p_{c1} = \frac{Y_0}{k\alpha}\left[\left(\frac{\alpha}{\alpha - 1}\right)^{2k/3} - 1\right], \tag{7}$$

where Y_0 and k are the adhesion and the friction coefficient in the Mohr–Coulomb law,

$$\tau_1^2 = \frac{\rho_{0m} a_0^2}{3Y_0(\alpha_0 - 1)^{2/3}}, \quad Q_1 = \ddot{\alpha}\frac{[1 - (\alpha/(\alpha-1))^{(2k+1)/3}]}{\alpha^{1/3}(2k+1)} - \dot{\alpha}^2\frac{[1 - (\alpha/(\alpha-1))^{(2k+4)/3}]}{3\alpha^{4/3}(k+2)},$$

and a_0 is the characteristic pore size. The condition $p = p_{c1}$ serves as a criterion of failure for brittle bulk materials in compaction.

Failure in the mobile and immobile punches and in the compacted powder, which is caused by interaction of counter unloading waves, is regarded as the process of discontinuity growth under the action of tensile stresses. The limiting value of the specific volume of voids $\xi^* = (\alpha^* - 1)/\alpha^*$ is a criterion of material failure in this approach [5]. The process of pore growth in a plastically deformed material is described by the relations

$$\dot{\alpha} = 0, \quad p_c \leqslant p \leqslant 0;$$

$$\sigma_{sm}\tau^2 Q(\alpha, \dot{\alpha}, \ddot{\alpha}) = a_s \ln\left(\frac{\alpha}{\alpha - 1}\right) + \alpha p + \frac{2}{3}\dot{\alpha}\frac{\eta}{n}\frac{[\alpha^n - (\alpha-1)^n]|\dot{\alpha}|^{n-1}}{\alpha^n(\alpha-1)^n}, \tag{8}$$

$$p < p_c = -\frac{a_s}{\alpha}\ln\left(\frac{\alpha}{\alpha - 1}\right).$$

Here $\tau^2 = \rho_{0m} a_0^2/(3\sigma_{sm}(\alpha_0 - 1)^{2/3})$ and $Q(\alpha, \dot{\alpha}, \ddot{\alpha}) = -\ddot{\alpha}[(\alpha-1)^{-1/3} - \alpha^{-1/3}] + (1/6)\dot{\alpha}^2[(\alpha-1)^{-4/3} - \alpha^{-4/3}]$, and η, n, and a_s are the experimentally determined constants.

The failed material is modeled by a bulk medium that is subject only to compression and does not withstand tensile stresses. Test calculations of shock-wave compaction of porous aluminum and iron and also of corundum ceramics powder have shown that system (1)–(8) describes satisfactorily the shock adiabats of porous and bulk materials for $\alpha_0 \leqslant 2$. For the case of zirconium dioxide powder ($\alpha_0 = 14$) whose particles in

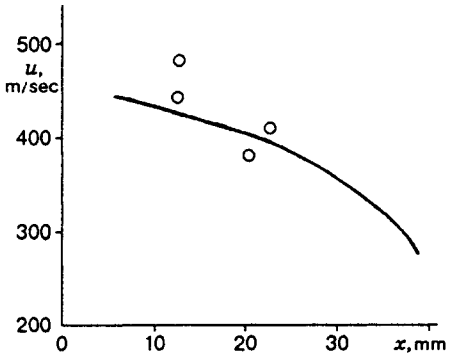

Fig. 2

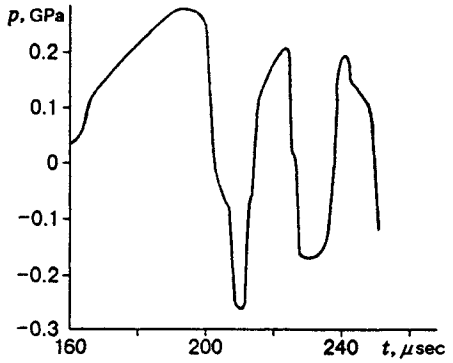

Fig. 3

the initial state have the shape of void spheres, it is assumed that powder compaction at the initial stage of compaction is caused by failure of the particle shells and by a decrease in the porous space. Therefore, the material pressure is related to the condition of failure of the powder particles:

$$p = \frac{Y_0}{k\alpha}\left[\left(\frac{\alpha}{\alpha - 1}\right)^{2k/3} - 1\right], \quad \alpha = V\alpha_0. \tag{9}$$

Under initial and boundary conditions corresponding to the experimental conditions, system (1)–(9) is solved by the numerical method given in [6].

Discussion of the Results. We realized several variants of computer simulation of shock compaction in a rigid matrix of zirconium dioxide powder with a bulk density of 0.43 g/cm^3. The impact velocity in the calculations was varied within the range 0.3–2 km/sec (the thickness of the mobile punch was 0.33 cm, the thickness of the immobile punch was 2 cm, and the height of filling was 5.16 cm). The constants in the condition of powder-particle fragmentation were found from a comparison of the numerical and experimental results. We used the same shock adiabat of zirconium dioxide of crystalline density as that in [7]. The final density of the compacts extracted from the conservation ampoule after shock-wave compression served as a reference point for the final stage of compaction. At the initial stage of a single compression the calculations were compared with the kinematic parameters of the powder in flow, which were measured by needle sensors.

In Fig. 2, the calculated and measured velocities of the striker–mobile punch system are compared as a function of the distance x passed in the ampoule. The boundary conditions of the problem corresponded to the experimental design, in which the velocity of the striker was 600 m/sec, the total mass of the striker and of the driving device was 35 g, and the powder mass was 10 g. Satisfactory agreement of the data for the punch-velocity decay, which was observed in all the variants of calculation, confirms that the one-dimensional approximation is applicable when compaction in a passing compression wave is considered.

The distributions of stresses and of the relative volume of voids at various moments of time, which were obtained in the calculations, make it possible to analyze the evolution of the stress-strain state in the sample and the degree of compaction and fracturing of the compact. The onset of the process is characterized by propagation of shock waves from the contact surface of the striker and the mobile punch. In the mobile punch, after the shock front comes to the contact boundary with the sample, it splits into an elastic compression wave traveling to the powder and an elastoplastic unloading wave reflected into the shock-compressed material of the mobile punch. In this case, the interaction of counter rarefaction waves can lead to spalling of the striker.

From the calculation it follows that, for example, a steel striker 6 mm thick remains intact at an impact velocity of 500 m/sec, and when the velocity is doubled, it separates into two parts. Separation of the striker in this range of impact velocities is confirmed by the experiments performed. It should be noted that owing to the low bulk density of the powder (the relative volume of voids is 92%), the wave pattern occurring in the striker and in the mobile punch does not have a substantial influence on the compaction process; only their masses and the initial rate of interaction are important.

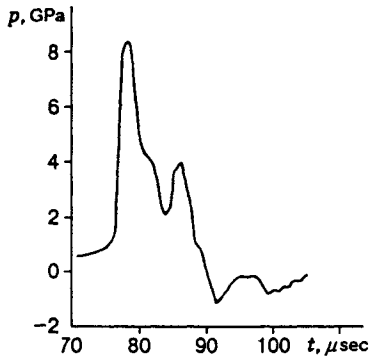

Fig. 4

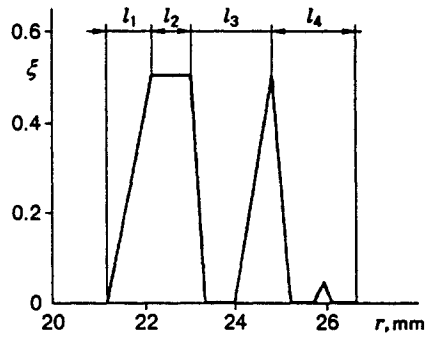

Fig. 5

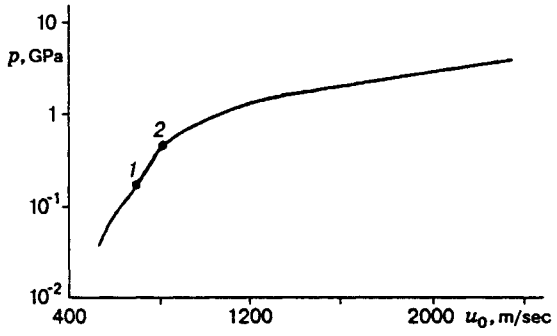

Fig. 6

As the striker moves into the ampoule, the mass velocities in the striker and in the mobile punch are equalized. The shock front in the powder, which is also the failure front of the material particles, is adjacent to the surface of the mobile punch. As the elastic compression wave in the powder reaches the surface of the immobile punch, it breaks down into a compression wave traveling toward the material of the immobile punch and a compression wave reflected to the powder. Reflecting from the surface of the immobile punch and the shock front, the latter wave, in turn, increases the level of compressing stresses in the space between them and leads to a decrease in the relative volume of the voids. When the impact velocity is 500 m/sec, the shock-wave compaction lasts 200 μsec. By this time, the mobile punch stops moving. The materials of the mobile and immobile punches are subject to the action of compressing stresses. The relative volume of the voids in the compacted preform reaches 0.2. In 250 μsec after the impact, the materials undergo the action of tensile stresses, but their magnitude is insufficient for growth of micropores.

Figure 3 shows the time dependence of pressure at an impact velocity of 500 m/sec for a fixed plane located before the onset of compaction at a distance of 24 mm from the surface of the immobile punch. In the process of compaction, the distance between these planes reduced to 2.7 mm. In 160 μsec, the relative volume of the voids in the material in this plane is equal to 0.53, and the level of compressing stresses reaches 30 MPa. As the compaction proceeds, the level of compressing stresses increases to 275 MPa in 190 μsec, and we observed this value approximately 10 μsec. After that, it decreases owing to the interaction of counter unloading waves. The relative volume of the voids decreases to 0.2 for this period, and the sample begins to undergo the influence of tensile stresses, whose maximum value at instant 210 μsec is equal approximately to 270 MPa. The subsequent loading and unloading of the sample do not lead to variation in material porosity.

From the calculations it follows that an increase in the impact velocity leads to a decrease in the compaction time. At an impact velocity of 1000 m/sec, the complete compaction of zirconium dioxide powder occurs already in 80 μsec. Starting with this moment, the velocity vector of the mobile punch is opposite to the impact direction.

Figure 4 gives the time dependence of pressure in a plane at a distance of 24 mm from the immobile-punch surface, as in the previous variant. With the complete compaction, this plane is at a distance of 2 mm from the surface of the immobile punch. An increase in the impact velocity leads to an increase in the shock-wave amplitude in the powder, but the maximum pressures in this wave are realized at the mobile-punch surface, as in the case where the impact velocity is reduced by one half. Intense fragmentation of the powder particles occurs until the relative volume of the voids reaches a value of 0.5. The maximum calculated level of compressing stresses in the powder at this impact velocity is 8.3 GPa. At this moment, the thickness of the compacted preform is 3.5 mm. The interaction of the counter unloading waves propagating from the mobile and immobile punches leads to lamination of the preform.

Figure 5 shows the distribution of the relative volume of voids over the thickness of the sample by the moment 120 μsec. It is assumed in the calculations that failure will occur in an element of the compressed material if the relative volume of voids in it reaches 0.5, as a result of the action of tensile stresses. The local lamination corresponds to that observed experimentally: the compacted preform separates into four layers, whose thickness l varies within a range of 0.7–1.7 mm. The final thickness of the compact is approximately 5 mm, as that in the experiment.

The calculated peak pressure in the zirconium dioxide powder versus the impact velocity is presented on a semilogarithmic scale in Fig. 6. Point 1 corresponds to the complete compaction of the material and point 2 corresponds to the lower boundary of compact lamination.

A comparison of the data of computer simulation with the experimental data has shown that the mathematical model described above can be used to analyze the processes in powder materials upon shock-wave treatment. The measurement and calculation data make it possible to relate the parameters of shock loading to the properties of modified ultradispersed zirconium dioxide at various structural levels.

This work was supported by the Russian Foundation for Fundamental Research (Grant 95–01–00713a).

REFERENCES

1. V. F. Tatsii, A. V. Anan'in, O. N. Breusov, et al., "The properties and sintering of SHS powders of titanium carbide activated by shock-wave action," in: *Papers of IV All-Union Meeting on Detonation* [in Russian], Telavi (1988), Vol. 2, pp. 47–53.
2. S. N. Kul'kov, V. F. Nesterenko, M. P. Bondar', et al., "Activation of rapidly hardened submicron ceramic ZrO_2–Y_2O_3 powders by explosion," *Fiz. Goreniya Vzryva*, **29**, No. 6, 66–72 (1993).
3. L. V. Altshuler, G. S. Doronin, and S. V. Klochkov, "A method for determining shock adiabats of low-density materials," in: *Abstracts of 1st All-Union Symp. on Macroscopic Kinetics and Chemical Gas Dynamics* [in Russian], Alma-Ata (1984), Vol. 1, Part 1, pp. 31–32.
4. I. Birkby, P. Harrison, and R. Stevens, "The effect of surface transformation on the wear behavior of zirconia (TZP) ceramics," *Ceram. Eng. Sci. Proc.*, **9**, Nos. 9 and 10, 782–786 (1988).
5. N. N. Belov, A. I. Korneyev, and V. G. Simonenko, "A model of spalling of a porous elastoplastic medium experiencing a polymorphous phase transition," *Dokl. Akad. Nauk SSSR*, **310**, No. 5, 1116–1120 (1990).
6. M. L. Wilkins, "Elastoplastic flow calculation," in: *Calculation Methods in Hydrodynamics* [Russian translation], Mir, Moscow (1967), pp 212–263.
7. D. Grady, "Shock wave properties of high-strength ceramics," in: *Shock Compression of Condensed Matter*, Elsevier, New York (1991), pp. 455–458.